Heliyon 9 (2023) e14538

Contents lists available at ScienceDirect

Heliyon

journal homepage: www.cell.com/heliyon

Research article

One-pot green synthesis of silver nanoparticles using brittle star *Ophiocoma scolopendrina*: Assessing biological potentialities of antibacterial, antioxidant, anti-diabetic and catalytic degradation of organic dyes

Ida Elizabeth George [a], Tijo Cherian [a,**], Chinnasamy Ragavendran [b], R. Mohanraju [a], Hamad Ghaleb Dailah [c], Rym Hassani [d], Hassan A. Alhazmi [e], Asaad Khalid [e,f], Syam Mohan [e,g,h,*]

[a] *Department of Ocean Studies and Marine Biology, Pondicherry University, Port Blair Campus, Brookshabad, Port Blair, 744112, Andaman*
[b] *Department of Conservative Dentistry and Endodontics, Saveetha Dental College and Hospitals, Saveetha Institute of Medical and Technical Sciences (SIMATS), Chennai, India*
[c] *Research and Scientific Studies Unit, College of Nursing, Jazan University, Jazan, 45142, Saudi Arabia*
[d] *Department of Mathematics, University College AlDarb, Jazan University, Jazan, Saudi Arabia*
[e] *Substance Abuse and Toxicology Research Center, Jazan University, P. O. Box: 114, Jazan, 45142, Saudi Arabia*
[f] *Medicinal and Aromatic Plants and Traditional Medicine Research Institute, National Center for Research, P. O. Box 2404, Khartoum, Sudan*
[g] *School of Health Sciences, University of Petroleum and Energy Studies, Dehradun, Uttarakhand, India*
[h] *Center for Transdisciplinary Research, Department of Pharmacology, Saveetha Dental College, Saveetha Institute of Medical and Technical Science, Saveetha University, Chennai, India*

ARTICLE INFO

Keywords:
Ophiocomascolopendrina
Brittle star
Silver nanoparticles
Antibacterial
Antioxidant
Antidiabetic
Catalytic activity
Organic dyes

ABSTRACT

In the current study, aqueous extract of *O. scolopendrina* (OSE) was used to synthesize AgNPs in a simple and environmentally friendly manner. The biosynthesized OSE-AgNPs were also assessed for its catalytic, antibacterial, anti-diabetic, antioxidant and dye degradation properties. The techniques like UV–visible spectroscopic examinations, TEM, SEM, TGA, zeta potential and FT-IR were used in the characterization investigations. The bioproduction of OSE-AgNPs was preliminary confirmed by UV–visible spectroscopic based investigation followed by microscopic visualization. The synthesized OSE-AgNPs exhibited a reddish brown colour and nearly spherical forms with sizes between 5 and 50 nm quantified by TEM and SEM. The attendance of functional groups like –OH and –NH present in OSE caps on the AgNPs surface was confirmed by FTIR analysis. Interestingly, in the presence of OSE-AgNPs, the degradation of dyes (CV, 95% and EY, 96% in 15 min) were noticeably accelerated. Further, OSE-AgNPs demonstrated substantial antibacterial activity; robust antioxidant properties andnotable anti-diabetic activities. This is the first account on the biosynthetic process of AgNPs using the aqueous extract of *O. scolopendrina*.

* Corresponding author. Substance Abuse and Toxicology Research Center, Jazan University, P. O. Box: 114, Jazan, 45142, Saudi Arabia.
** Corresponding author. Department of Ocean Studies and Marine Biology, Pondicherry University, Port Blair Campus, Brookshabad, Port Blair, 744112, Andaman.
E-mail addresses: tvarghese891@gmail.com (T. Cherian), syammohanm@yahoo.com (S. Mohan).

https://doi.org/10.1016/j.heliyon.2023.e14538
Received 24 December 2022; Received in revised form 1 March 2023; Accepted 10 March 2023
Available online 16 March 2023

1. Introduction

The recent advances in nanosciences have resulted in an explosion of scientific research areas with a focus on the study of nanoparticles and the use of biological sources in the green manufacture of nanoparticles [1,2]. The conception of different metal and metal-based nanoparticles has gained tremendous research interest over the past years due to its unique properties in nanotechnology, such as electrochemical, energy, imaging, catalysis, and biomedical properties [3–5]. Metal based NPs can be made and stabilized using a variety of methods, including environmentally friendly, chemical and physical ones. Among these, chemical and physical techniques involved poisonous substances, unsteady, required numerous processes and high temperatures and pressures [6]. These unsustainable metal nanoparticles were also unsuitable for use in medicinal applications, such as drug delivery, antidiabetic, and anticancerous properties. The synthesis of metal nanoparticles using green technologies is creative, low-cost, and occurs under mild reaction conditions.

Silver, a harmless inorganic antibacterial agent that is non-toxic and well known for its ability to kill over many different types of disease-causing microbes has been used for millennia [7]. The ability of silver to exert a substantial potential for a variety of biological applications, including prevention of infections, wound healing, and acting as an anti-inflammatory even at very low concentrations, has led to the description of silver as being oligodynamic. Due to their antibacterial properties, silver ions (Ag^{+}) are used in the manufacture of bone cement, dental resin composites, ion exchange fibres, and coatings for medical equipment's. Recent research has demonstrated that the majority of microorganisms, such as bacteria, fungi, viruses, and some pathogens, are strongly inhibited by silver nanoparticles [8].

Several studies have been published that describe the synthesis of metal nanoparticles using various plant-based materials, such as flowers, leaves, roots, stems, bark, fruit, buds, and latex in the green approaches for the fabrication of AgNPs. According to recent publications, numerous investigations have been conducted to investigate the role of the implicated phytochemicals in the green synthesis and stability of AgNPs via phyto-based materials [9,10]. These phytochemicals were identified by the various spectroscopic analyses as being the most crucial in the biological reduction of Ag^{+}in AgNPs from Ag(I) to Ag(0) [11,12]. In actuality, the constituents of extracts function as possible capping and reducing agents [13,14]. They limit the agglomeration of nanoparticles and prevent their overgrowth during colloidal production. By making these molecules more functionally ideal for various applications, they can also affect and customize the characteristics of the biomanufactured nanoparticles [15]. Due to surface plasmon resonance, AgNPs generally demonstrated strong catalytic and biological applications [16]. In most cases, by synthesizing the nanoparticles with unique molecules such as sugars, proteins, fibres, vitamins, polymers, and ligands, in addition to components other than those obtained from plants, it is possible to control and regulate the growth and formation of agglomeration [17,18]. Additionally, the specific design, size, and shape of the silver nanoparticles were carried out using these phyto-based components as stabilizers and reducers [3]. Till date, there is currently no published research on the production of AgNPs by the aqueous extract of marine species of brittle star.

Non-biodegradable organic dyes produced by the textile, plastic, paper, and food sectors are frequently dumped in water without any prior treatment, posing a serious environmental pollution problem [19]. Many of these dyes are highly harmful to human life and have mutagenic and carcinogenic effects, which can significantly harm aquatic organisms. As a result, dye effluents need to be treated in order to get rid of these substances from waste waters. Traditional methods used for this purpose include absorption, chemical, photochemical, and bio-degradative approaches [20]. Due of their great chemical stability, dye pollutants are relatively resistant to these physical-chemical techniques. As worldwide environmental safety requirements are getting more and more rigorous, it is important to remove these harmful chemicals from these wastewaters [21]. To this goal, a range of treatments have been proposed and developed, including biological and physico-chemical approaches. An optimal dye removal process must be able to remove a lot of dye quickly and efficiently without adding to pollution by generating more dangerous by-products. To this purpose, a lot of research has been done on the use of environmentally friendly synthetic metallic nanoparticles as effective catalytic agents in the reduction of organic pigments [22]. Metal nanoparticles are recommended as effective catalysts for the reductive degradation of organic dyes due to their distinctive electrical, physical, and chemical properties. This makes them an efficient alternative to current methods for removing dye impurities. Silver nanoparticles made from green synthetic materials are widely utilized presently to remove dyes from aqueous medium [20].

In light of this, we developed a straightforward, economical, green synthesis of AgNPs stabilized by the aqueous extract of *Ophiocoma scolopendrina* underlying the principles of green chemistry. The principles of "less hazardous chemical synthesis" and "inherently safer chemistry" were followed as the aqueous form of extract and use of a biological species were employed for the synthesis of environmentally benign and safe nanoderivatives in asustainable and economical manner. The present study qualifies the practicing green chemistry approaches under bottom-up module by the use of benign aqueous extract of *O. scolopendrina* reported for the first time in the synthesis of AgNPs. The morphological features and SPR effect were determined by using characterization techniques of TEM, SEM, FTIR, UV–Vis absorption spectra, etc. For biological degradation and reduction of dyes in the presence of $NaBH_4$, OSE-AgNPs demonstrated exceptional catalytic activity. Additionally, the OSE-AgNPs were employed to gauge the screening of antibacterial, anti-diabetic properties, antioxidant DPPH(2,2-diphenyl-1-picrylhydrazyl)and ABTS (2,2-azinobis-3-ethylbenzothiazoline-6-sulphonic acid)scavenging activities, and the outcomes were compared with standard compounds.

2. Material and methods

2.1. Chemicals

Sodium borohydride ($NaBH_4$), silver nitrate ($AgNO_3$), potassium bromide (KBr), dyes crystal violet (CV) and eosin Y (EY) were

purchased from HiMedia.

2.2. Collection of brittle star

The specimen of brittle star (*Ophiocoma scolopendrina*) was collected from the intertidal region of Burmanallah(11°34′22.26″N, 92°44′22.51″E), South Andaman, India in a refrigerated box and transferred to the laboratory. The sample was cleaned using autoclaved marine water to get rid of any clinging debris and related biota before being sterilized and stored. The taxonomic identification of the organism was done by using taxonomic identification keys [23]. The voucher specimen was deposited at Marine Microbiology laboratory under register no. MM0117.

2.3. Extract preparation (OSE) and synthesis of silver nanoparticles

The biosynthesis of silver nanoparticles was carried out by ultrasonication method [24] using the aqueous extract of brittle star. The dry powdered sample of brittle star was prepared by shade drying the collected organism. Five grams of brittle star sample (dry state) was grounded in 30 ml sterile deionized water by using pestle and mortar. Post thorough grinding, the resulting crude extract was strained by using Whatman No.1 (pore size 11 μm) filter paper. The filtrate (10 ml) + 90 ml of aqueous 10^{-3} M silver nitrate ($AgNO_3$) solution was mixed and kept in an ultrasonic bath with a volume of 2.0 l water at 50 °C. Because of ultrasonication, the water temperature was elevated slightly, adjusted and maintained at 50 °C ± 2 °C during the entire synthetic process. The bio-reduction (99%) of $AgNO_3$ formed to black confirming the silver bio-reduction through visual observation.

2.4. Purification of silver nanoparticles

In order to remove unbounded phytomolecules, the biosynthesized OSE-AgNPs were washed by centrifugation at 10,000 rpm for 15 min. The sample of pure silver nanoparticles was dried in an oven at 50 °C and used in subsequent investigations.

2.5. Characterization of biogenic silver nanoparticles

The analytical methods were used to determine the physicochemical properties of OSE-AgNPs: TEM (transmission electron microscopy); SEM (scanning electron microscopy); UV–visible spectrophotometry; zeta potential analysis; thermogravimetric analysis (TGA); and Fourier transform infrared spectroscopy (FT-IR). In addition to operating considerations, all characterization approaches, were put into practice in accordance with prior reports of [25,26].

2.6. In-vitro antioxidant assays

2.6.1. DPPH radical-scavenging activity

The colour bleaching sensitivity of 2,2-diphenyl-1-picrylhydrazyl (DPPH) in methanol was used to test the electron-donating capacity (or hydrogen atom) of OSE-AgNPs [27]. A total of 50 μl of OSE-AgNPs(concentrations 20–100 μg/ml) were mixed separately with 450 μl of Tris-HCl buffer (pH = 7.4) and 1 ml of methanolic DPPH solution (0.1 mM) and incubated at room temperature in the dark for 30 min before measuring their respective absorbance values at 517 nm. Ascorbic acid and methanol were employed as the standard and blank, respectively. The inhibitory concentration (IC50 value) at which 50% (IC50) DPPH free radical scavenging activity of OSE-AgNPs was assessed. The equation (Eq. (1)) below was used to compute the percentage of DPPH radical inhibition:

$$Inhibition\ \% = \frac{([ABlank - Bsample])}{ABlank} \times 100 \quad (1)$$

where, A blank - the absorbance of the control reaction and B sample - is the absorbance of the test compound.

2.6.2. ABTS radical scavenging assay

In scavenging assay, ABTS reaction mixture consisting of 7 mM ABTS +2.45 mM$K_2S_2O_8$ (potassium persulfate) was incubated for 12 h at 27 °C under dark conditions. Additionally, by dilution with methanol, the OD (optical density) of reaction solution was adjusted to 0.7 at 734 nm. Following, the different concentrations of OSE-AgNPs (20–100 μg/ml) were added to 3 ml reaction solution and incubated at 27 °C under dark for 6 min. The optical density was quantified at 734 nm. Ascorbic acid served as the reference solution and the reaction solution without the test sample served as control.

2.7. In-vitro anti-diabetic studies

2.7.1. α-amylase inhibitory activity

The α-amylase inhibitory activity of OSE-AgNPs was carried out using standard procedure with slight modifications [28]. In 96-well plate, 20 μl α-amylase (2 U/ml) + 20 μl OSE-AgNPs(20–100 μg/ml) were mixed with 50 μl phosphate buffer (100 mM, pH 6.9) and incubated for 20 min at 37 °C. Following then, a substrate solution of soluble starch (1%, 20 μl; 100 mM phosphate buffer pH 6.9) was mixed; incubated at 37°C for 30 min. Post incubation, DNS color reagent (100 μl) was added; boiled for 10 min and the absorbance

was read at 540 nm. Standard (acarbose) and control mixtures were ran in parallel as control. The results were interpreted as % inhibition calculated by using equation (Eq. (2)):

$$\text{Inhibitory activity } (\%) = \left(1 - \frac{A}{B}\right) \times 100 \tag{2}$$

where A = absorbance of test sample and B = absorbance of control.

2.7.2. α-glucosidase inhibitory activity

All other experimental sample preparations, apart from the approach of [29], followed the instructions mentioned in section 2.7.1.

2.8. Mechanism of action of SCE-AuNPs on microbial cells

2.8.1. Protein leakage assay

The methods of [30]were used to determine the quantification of protein constituent leakage. After being exposed to OSE-AgNPs (100 μg/ml) for 3–6 h, the bacterial cells were centrifuged (6000 rpm; 15 min). The supernatant (200 μl) and Bradford reagent (800 μl) were added to each consecutive sample before being incubated for 10 min. The absorbance (at 595 nm) was determined using BSA (Bovine Serum Albumin) as a reference.

2.8.2. Nucleic acid leakage assay

The previously described standard technique of [31] with minor adjustments was used to estimate nucleic acid leakage. Aliquots of bacterial cultures were mixed with OSE-AgNPs (100 μg/ml)) for intervals of 3–6 h, post exposure were filtered through syringe filters (pore size of 0.2 μm; diameter 25 mm; Millex-GS, Spain). The absorbance was measured at 260 nm.

2.9. Antibacterial activity

The antibacterial property of OSE-AgNPs was investigated by using agar well diffusion assay against Gram-positive(*Staphylococcus aureus*MTCC 96) and Gram-negative (*Escherichia coli*O157:H7VT3) bacteria [32]. In brief, the MHA medium plates were uniformly swabbed with 100 μl of pre-grown bacterial culture. Wells (10 mm in size) were made by using sterilized cork borer and the former were then subsequently filled with OSE-AgNPs (20–100 μg/ml) and incubated for 24 h at 37 °C.The OSE alone and ampicillin (positive control)were run as parallel setups. The formation of inhibitory zone around the wells on each plate was measured by using HiMedia antibiotic ZOI scale [26].

2.10. Catalytic degradation of organic dyes

The OSE-AgNPs, in the presence of $NaBH_4$, were employed to study the catalytic degradation kinetics of organic dyes:eosin Y (EY, $\lambda = 516$ nm) and crystal violet (CV, $\lambda = 584$ nm). A unique method was used to produce the final colloidal suspension consisting of OSE-AgNPs (1 ml)+ mixture of dye stock solution (10 mM) and freshly prepared solution of $NaBH_4$(3 ml; 10 mM). To create a homogeneous solution, it was kept at a water bath with ultrasound treatment while being constantly stirred. The reaction mixture was continuously stirred while being irradiated to facilitate the catalytic breakdown of dyes. A little amount of the solution (0.5 ml) during the reaction was obtained and recorded UV–Visible spectrophotometer at regular intervals (3 min). The progression of degradation process was tracked over time, and the long-lasting absorbances of dyes at corresponding wavelengths were noted. For comparative purposes, the control sets of pure dyes without catalyst (OSE-AgNPs) were also ran parallel and along with an evaluation of degradation under the same reaction circumstances. The following equation (Eq. (3)) was used to estimate the proportion of dye degradation using OSE-AgNPs:

$$\textit{Degradation efficiency } (\%) = \frac{(Ao - At)}{Ao} \times 100 \tag{3}$$

where, A_0 = initial absorbance of dye; A_t = absorbance of dye at time t.

2.11. Statistical analysis

Data are displayed as mean S.D. With the use of the statistical analysis program Sigmaplot 10.1, differences between groups were ascertained using a one-way ANOVA. The p value < 0.05 was used to conclude significant differences.

3. Results and discussion

The morphology of samples has a significant impact on the intriguing optical characteristics of silver nanostructure, which are closely related to SPR (surface plasmon resonance). The most popular tool for studying the SPR is UV–visible absorption spectrophotometer. The aqueous extract of brittle star (OSE) was used to synthesize AgNPs, and the UV–visible spectroscopic analysis was used to observe the sharp and intense SPR peaks. The intensity of the absorption band was found to be promising as results of the

formation of highly disperse nanoparticles. The successful creation of silver nanoparticles, as well as the regulation of their size and distribution, was discovered to be influenced by the solvent employed for extract synthesis [33]. The biological metabolites found in the extract play a substantial impact in the size, shape, and optical properties of silver nanoparticles [33]. At the beginning of the synthesis procedure, 10^{-3}MAgNO$_3$solution with brittle star extract (OSE) was used to produce AgNPs in a ratio of 1:9, along with 0.01 M AgNO$_3$solution devoid of OSE was kept as a control. The reaction solution changed colour within 30 min of reaction from yellowish-brown to reddish-brown, visually confirming the biological reduction of AgNO$_3$ into AgNPs (Fig. 1a). After the addition of the aqueous AgNO$_3$ solution, the colour of OSE turned turbid, signaling the start of the reaction. The synthesis of OSE-AgNPs was confirmed by the characterization of silver nanoparticles based on SPR (surface plasmon resonance) peak seen at 430 nm. Additionally, the biosynthesized OSE-AgNPs exhibited stability over a longer period of time (6 months) (Fig. 1b). It is common knowledge that the SPR phenomenon of silver metal nanoparticles causes AgNPs to appear reddish-brown in water [34]. It shows that adding OSE to AgNO$_3$ solution causes the reduction of Ag^+ into Ag^0, resulting in the formation of silver nanoparticles. In particular, there was a striking deepening of colour that indicated the saturation of reaction within 30 min suggesting minimal agglomeration and good particle dispersion throughout the synthesis media [35]. The size, shape, and dielectric constants of the metal nanoparticles and that of the surrounding medium, all affects the width and frequency of the surface plasmon absorption [26]. The stable position of the absorbance peak at the appropriate wavelength revealed that the generated OSE-AgNPs were not aggregates since the OSE contains a

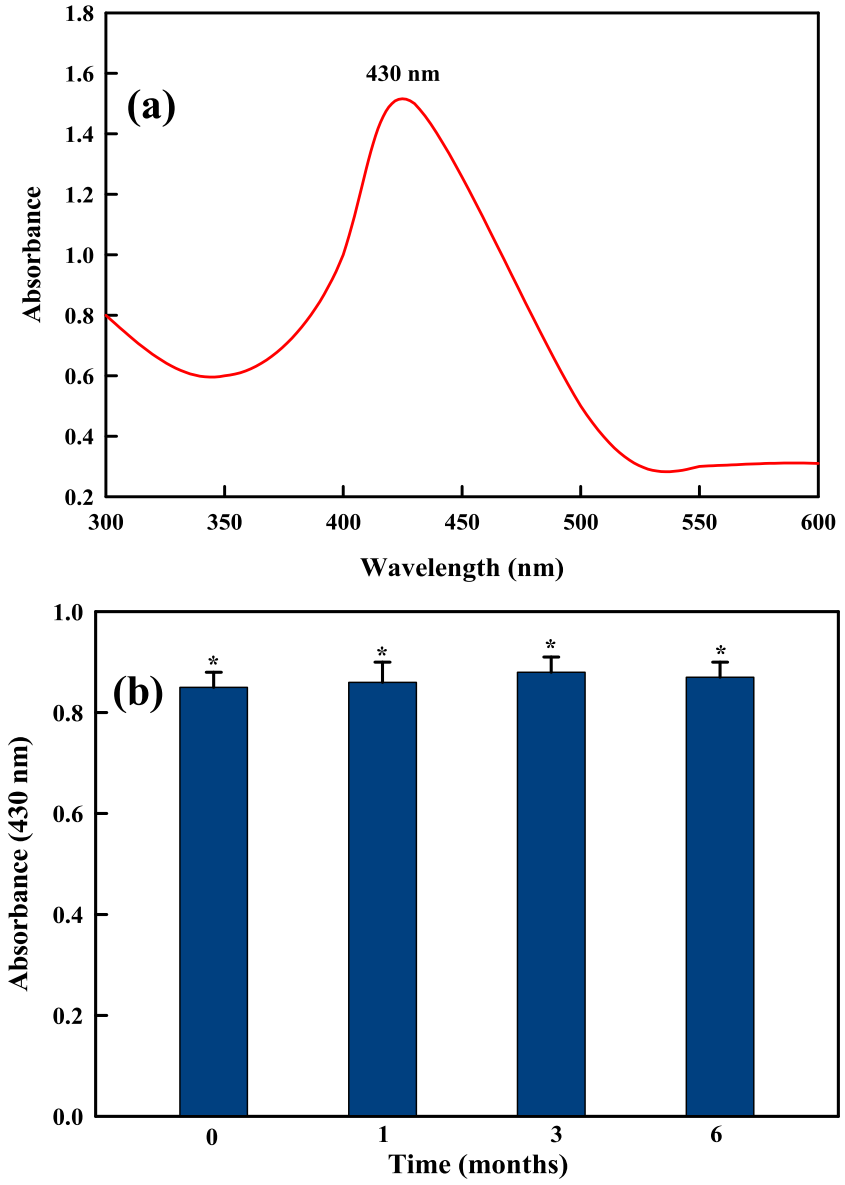

Fig. 1. Ultraviolet–visible (UV–vis) spectra of (a) OSE-AgNPs, (b) stability peaks recorded over time.

variety of biological organic moleculesthat are responsible for the reduction and stabilization of AgNPs which are well in accordance with previous reports of [26,34,36,37].

The electrical conversions between upper d-band and conduction sp-band are related to the photoluminescent characteristic of metallic NPs, such as AgNPs [38]. The recorded PL spectra (Fig. 2) of the synthesized OSE-AgNPs showed an emission peak (λ_{em} 430 nm)and an excitation wavelength (λ_{ex}322 nm); well in agreement with the previous reports of [37,38]. It results from the electronic excitation from the d-orbital into the upper Fermi level. When electrons were released from the sp-band to the holes from the d-band via the electron-phonon scattering process with energy loss, the synthesized OSE-AgNPs exhibited visible light responsive luminescence [38]. It was discovered that the emission properties of the generated OSE-AgNPs were affected by the inter-band and intra-band electronic transitions between two different electronic states. The piercingly increased PL intensity significantly improved the PL property of the synthesized OSE-AgNPs explicitly indicating the reduction of Ag by OSE.

The FTIR spectra were quantified in the identification of the likely functional groups involved in the biomolecules in OSE, which are responsible for effectively reducing and stabilizing the synthesized OSE-AgNPs(Fig. 3). The pronounced absorption peak at 3452 cm^{-1}corresponds to the –OH group of phenolic compounds [39]. The absorption bands at2926 and 2342 cm^{-1} were assigned to C–H aromatic stretch. In addition, the -C-C stretch vibrational peak at 1630 cm^{-1}indicated alkene group in the OSE-AgNPs [40]. The peak at1400 cm^{-1} was attributed to the N–H stretch of proteins in OSE [41]. Also, the peaks at 1113 and 1080 cm^{-1}were assigned to the vibrations of amide protein [42]. The absorptive peaks at 1152 cm^{-1} and422-1200 cm^{-1}assigned to -C-C and -C-N stretch of aliphatic amines in OSE, respectively. Finally, the presence of biomolecules like polyphenols, proteins in OSE is well sustained by these absorptive peaks of diverse groups, which are critical for the stability and reduction of OSE-AgNP [9–11]. Furthermore, the synthesized OSE-AgNPs may also consist of main constituents from the aqueous OSE based on the similarity of the FTIR spectra with significant wavenumber and intensity shifts between OSE and synthesized OSE-AgNPs.

The evaluation of various physical and chemical properties of synthesized OSE-AgNPs necessitates a thorough research of their morphology, shape, and diameter. TEM and SEM images at various magnifications were used to examine the surface morphology and diameter of OSE-AgNPs, and the resulting findings are shown in Fig. 4. The TEM image of OSE-AgNPs revealed their monodisperse in nature, with a regular spherical shape of variable size (Fig. 4a and c) and a mean diameter of 5–50 nm (Fig. 4b). This dispersity may be caused by the capping and stabilization of OSE as well as the ultrasonication effect [43]. The OSE-AgNPs displayed an exceptional spherical shape and clustered in distribution (Fig. 4d). Because there was less aggregation and sedimentation in the solution, it was hypothesized that the OSE-AgNPs might have been enveloped by the capping of biological organic molecules present in OSE [43]. Silver nanoparticles become electronically connected when they aggregate, and this coupled system exhibits a dissimilar SPR than individual particles. The SPR usually shifts to a longer wavelength than the resonance of a single nanoparticle in the event of a multi-nanoparticle aggregate, and aggregation is detectable as an increase in intensity in the infrared area of the UV–visible spectrum [44]. Additionally, one of the variables affecting the aggregation rate of produced silver nanoparticles can be the drying factor of the silver nanoparticles [45].

The electrical potential between the bulk liquid in which a particle is floating and the inner Helmholtz layer close to its surface is known as the zeta potential (ζ). It is a measurement that depicts particle charge and provides a hint as to the colloidal system's possible stability. If all of the suspended particles have a strong negative or positive zeta potential, flocculation will not be a tendency. There is no force to prevent the particles from aggregation and flocculation, though, if their zeta potential is low. The concept of zeta potential

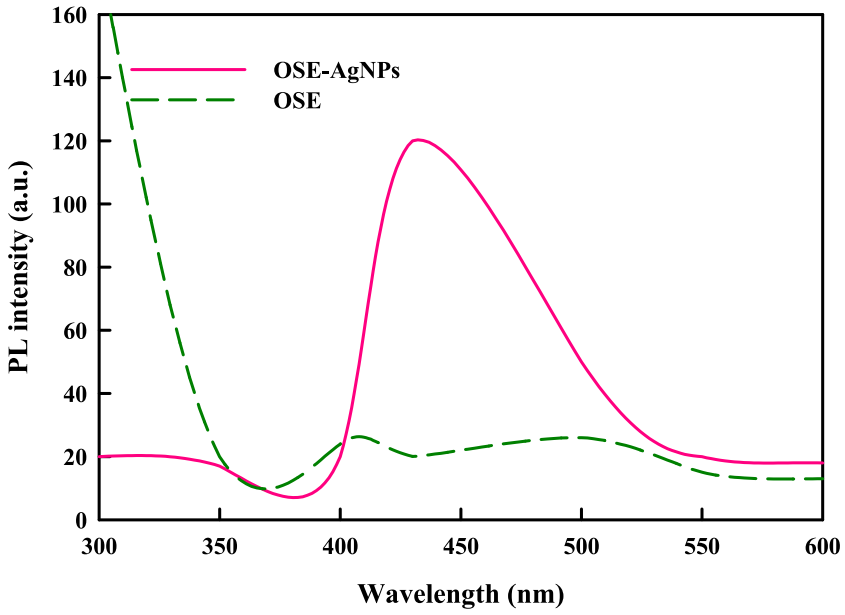

Fig. 2. PL spectra of the synthesized OSE-AgNPs and OSE.

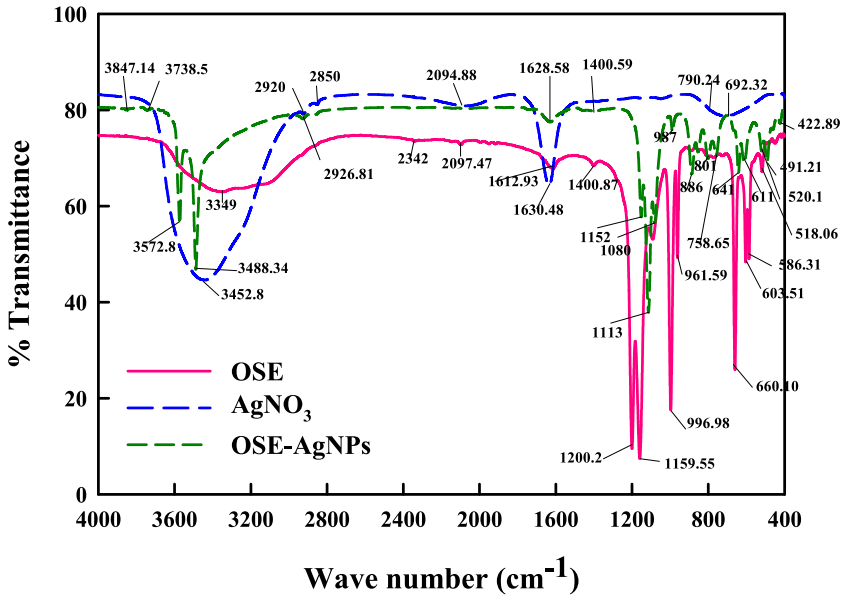

Fig. 3. FTIR spectra of the OSE, OSE-AgNPs, and $AgNO_3$.

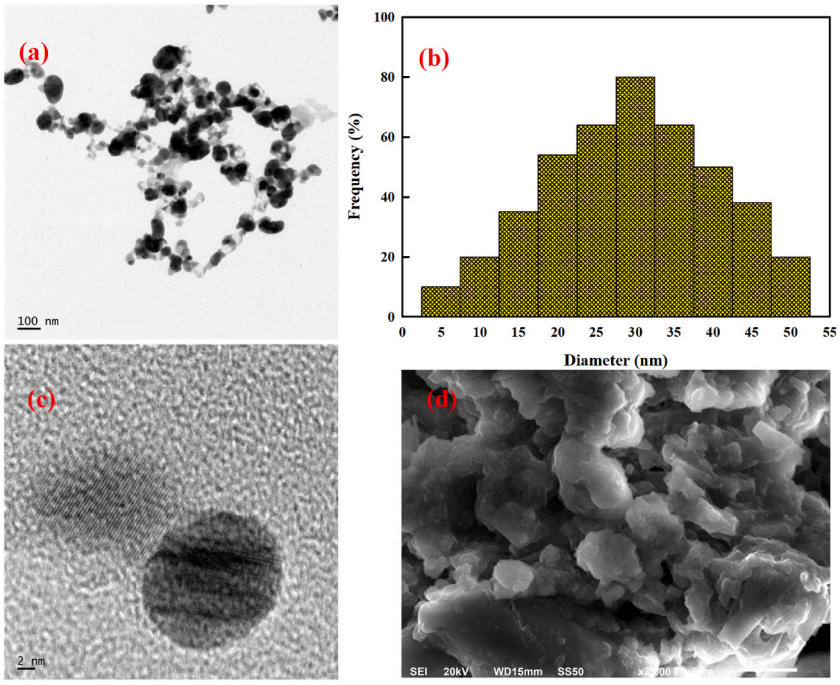

Fig. 4. Morphological analyses (a) TEM image at 100 nm, (b)size distribution histogram, (c) TEM image at 2 nm, and (d) SEM of OSE-AgNPs.

has been used to research cell adhesion, which is connected to surface charge properties, and is beneficial for comprehending and predicting the interactions and dynamics between particles in suspension [46,47]. The surface charge of the synthesized OSE-AgNPs was estimated using the zeta potential value (Fig. 5a) in order to measure the amount of charge and demonstrate the stability of the nanoparticles in dispersion by the creation of specific charge groups on their surface [48]. The result demonstrated that the AgNPs synthesized by aqueous extract of *O. scolopendrina* have a negative charge of −21.2 mV, probably as a result of adsorption of free ionic species; producing repulsion force as a factor of electrostatic stabilization [49]. The studies of [50,51] showed that the AgNPsfabricated with citric and tannic acid also exhibited negative charge. Further, the synthesized OSE-AgNPs was subjected to TGA assessment. The TGA was conducted in order to confirm the biological compounds capped on the surface of biosynthesized AgNPs [52,53]. For

studying a sample's heat stability and decomposition, the TGA is typically a reliable and effective method. The weight loss of the sample after heating is caused by the evolution of moisture and the breakdown of organic molecules [53]. The settled weight samples were heated at a rate of 100 °C/min from ambient temperature to 800 °C. Fig. 5b shows two distinct stages of the observed weight, with the underlying weight loss estimation from ambient temperature to 300 °C.Lower subatomic weight oligomers, moisture loss, and residual solvent can be attributed for the weight decrease up to this temperature. The second weight loss was observed at 400–600 °C implying the fundamental degradation of the biological molecules capped on the surface of OSE-AgNPs. The thermogravimetric analysis of OSE-AgNPs revealed a breakdown profile with a 400 °C to over 600 °C temperature range. This proved that the addition of Ag as a nanofiller improving the overall heat stability [54].

The biosynthesized nanoparticles are far more valuable in therapies than native metal nanoparticles due to their significant antioxidant capacity [55]. The ability of any substance to lessen the harm caused by the damaging oxidative stress resulting from an increase in the formation of reactive oxygen or nitrogen species (ROS/RNS) is referred to as antioxidant potential. The cellular oxidative and antioxidant systems become unbalanced as a result of this oxidative stress, which damages the tissue. For the evaluation of the antioxidant potential of nanoparticles, which helps to determine their suitability for various therapeutic applications, a variety of analytical approaches can be used. Most human diseases, including cancer and cardiovascular diseases appear to be characterized by the presence of free radicals, particularly by their increased production [56]. DPPH scavenging activity was assessed utilizing the environmentally friendly synthesized OSE-AgNPs at various concentrations of 20–100 μg/ml. The DPPH is frequently employed to investigate the capacity of different NPs to function as hydrogen donors or free radical scavengers [57]. The absorbance maxima at 517 nm gradually lower with the accompanying decolorization of the DPPH radicals when the odd electrons in the DPPH radicals are paired off in the presence of a reducing agent [58]. The DPPH radicals have an absorption peak at 517 nm because they have an odd number of electrons. As OSE-AgNPs give off protons and electrons, the stable DPPH radical can be reduced by giving hydrogen and electrons [58]. The synthesized OSE-AgNPs exhibited good DPPH scavenging activity (40–84%) in a standard in-vitro antioxidant assay under variable doses (20–100 μg/ml) (Fig. 6a). Based on a recent study, it may be assumed that the biomolecules present in OSE in OSE-AgNPs, high dispersion, and tiny particle size of nanoparticles, contributed to the favorable outcomes [59]. As a result, the ability of OSE-AgNPs to scavenge DPPH free radicals displayed exceptional scavenging activity. Furthermore, the OSE-AgNPs was analyzed for ABTS free scavenging test analysis. The ABTS assay, which is relatively new, uses a stronger radical that is chemically produced and is frequently used in the screening of complex antioxidant mixtures like plant extracts, beverages, and bodily fluids [60, 61]. The interest in using $ABTS^{\bullet+}$ for the estimation of antioxidant activity was sparked by its solubility in both organic and aqueous

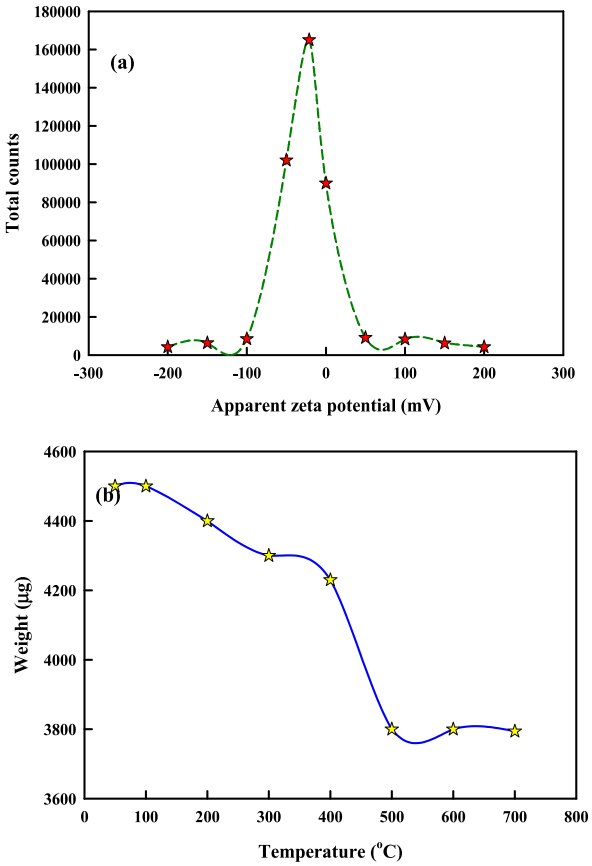

Fig. 5. Characterization of OSE-AgNPs. (a) Zeta potential, and (b) TGA.

media as well as its stability over a wide pH range [62,63]. The protonated radical $ABTS^{+\cdot}$ is thought to quickly receive an electron from an antioxidant molecule, changing its colour from blue to pink, observable at 734 nm [64]. At concentrations ranging from 20 to 100 μg/ml, the biologically synthesized OSE-AgNPs displayed an activity range of 32–84% in comparison to control BHT exhibiting 91–94% capacity to scavenge free radicals at various doses between 20 and 100 μg/ml, respectively (Fig. 6b). In earlier experiments of [65–67], the biologically synthesized AgNPs were reported to have a similar ABTS radical scavenging effect.

The green synthesized OSE-AgNPs were utilized for the assessment of in-vitro anti-diabetic activity using the α-amylase and α-glucosidase enzymes in a dose- and concentration-dependent manner (20–100 μg/ml). The results of OSE-AgNPs, when compared to those of the reference substance (acarbose), revealed noticeably moderate inhibitory activity (54% and 68%) in the enzymatic actions of both enzymes α-amylase and α-glucosidase (Fig. 7a and b). In accordance with earlier studies, the OSE-AgNPs boosted the rate at which glucose was utilized while decreasing the levels of an enzyme that is responsible for catalyzing the breakdown of carbohydrates [68,69].

The green-fabricated OSE-AgNPs demonstrated good antibacterial action against tested bacterial strains of *E. coli* and *S. aureus*. The MIC and MBC values evaluated were found to be 30–35 μg/ml and 60–70 μg/ml, respectively. It can be shown that the OSE-AgNPs, when comparable to ampicillin as control (not shown here), showed pronounced zones of inhibition (Fig. 8a and b). The inhibition zone of OSE-AgNPs against *E. coli* was found to be 21 ± 0.45 mm followed by 12 ± 0.6 mm in *S. aureus*. The Gram negative cells of *E. coli* was found to be more sensitive to OSE-AgNPs than the Gram positive cells of *S. aureus* as evident by the variability in the respective sizes of inhibition zone. Further, very less appreciable antibacterial activity was found in the case of OSE when applied alone inferring that the observed antibacterial activity was primarily due to nano-sized OSE-AgNPs. Additionally, the bacterial cells exposed to 100 μg/ml OSE-AgNPs displayed noticeably higher levels of protein and nucleic acid leakage ($p \leq 0.05$) than the control (Fig. 8c and d). In general, the interaction between the green produced OSE-AgNPs and the bacterial cell wall allowed the green OSE-AgNPs to demonstrate their antibacterial activity effectively. In addition, loss of proton motive force, protein denaturation, and cell death were used to produce the highest antibacterial activity [70]. Additionally, the particle size of OSE-AgNPs had an impact on whether the bacteria grew or were inhibited in their ability to do so. Although the exact mechanism underlying the bactericidal activity of AgNPs against bacterial cells is still unknown, several studies have hypothesized that the particles may adhere to the cell surface, disrupting vital processes including cellular respiration and cellular permeabilit y [71]. It is suggestive to know that how strongly the particles are linked to the bacteria depends on how much surface area is available for interaction. Particular nanoparticles enter the cell and attach

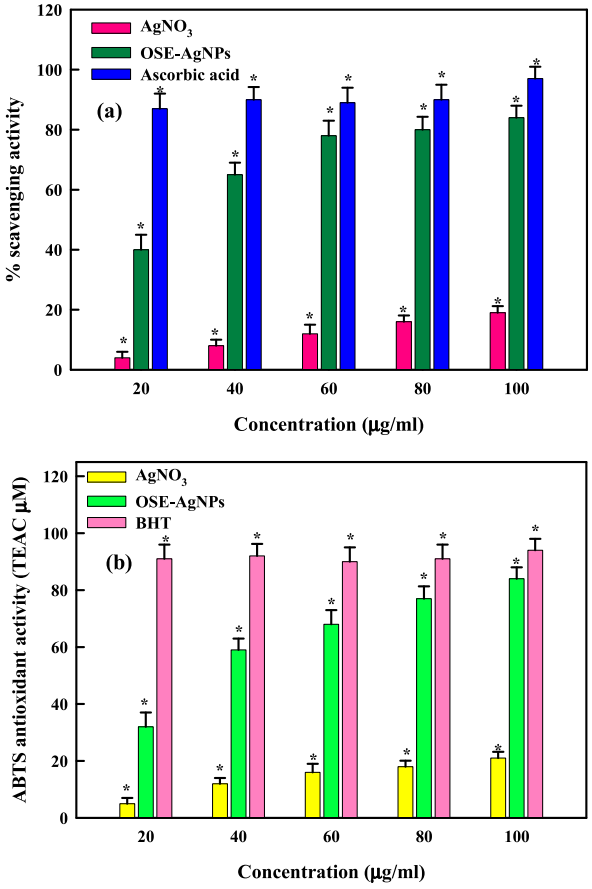

Fig. 6. In-vitro antioxidant activity of OSE-AgNPs (a) DPPH,and(b) ABTS assay.

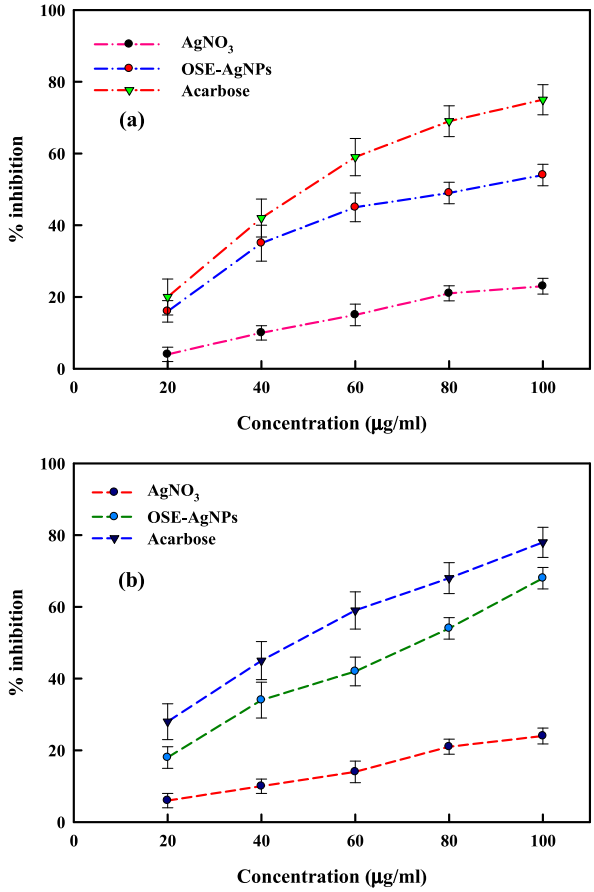

Fig. 7. In-vitro antidiabeticactivity of OSE-AgNPs, (a) α-amylase and (b) α-glucosidase.

to DNA, inhibiting the expression of some genes crucial to metabolism. Smaller particles, such nanoparticles, usually have a better bactericidal impact than bigger particles because they have a higher surface area to volume ratio that is available for contact [72]. Infectious disease treatment is severely hampered by the rise of resistant microorganisms to antibacterial drugs. Additionally, both gram-negative and gram-positive bacteria have increasingly developed novel strains with a worrisome level of resistance. In order to stop the establishment and spread of multi-resistant bacterial strains, there is a strong demand for the creation of new antibacterial chemicals [34].

The differential susceptibility of bacterial species towards nanoparticles toxicity also depends upon bacterial cell structure, degree of contact with NPs and particle size of NPs [73]. Several mechanisms have been documented on the mode of action of nanoparticles (Fig. 9). One of the postulate correspond to (1) the attachment of nanoparticles to negatively charged cell surface, thereby, altering the physical and chemical properties of the cell membrane and cell wall, leading to the destabilization of important functions such as (2) electron transport, osmoregulation, cell permeability and cell respiration [74,75]. (4) Another scheme put forwards an effective permeation of nanoparticles into the cell due to their nano-size, thereby interacting with DNA, proteins and protein-containing components [76]. Furthermore, (5) the release of metal ions from metal based nanoparticles causes cellular imbalance, thereby, triggering amplified biocidal effects [77].

The catalytic degradation of CV and EY dyes (10 mM, 10 ml) in the attendance of $NaBH_4$ (10 mM, 3 ml) was examined for the assessment of catalytic degradation efficiency of OSE-AgNPs (1 ml). First, the UV-absorptive peaks of aqueous solutions of dyes CV and EY at 584 nm and 516 nm, respectively, were measured. The maximum absorption pattern of CV and EY dyes was recorded by using UV–Vis spectrometer at the beginning of a reaction in the attendance of OSE-AgNPs (Fig. 10a and b). When a catalytic reaction using synthesized OSE-AgNPs was used to degrade dyes, the maximum absorption intensity steadily decreased over the course of the reaction period up to 15 min. In Fig. 11a, it is shown that less than 10% dye degradation occurs in the absence of a catalyst, while a near complete dye degradation only occurs in the attendance of $NaBH_4$and OSE-AgNPs. Finally, the maximum intensity of related absorption peak steadily decreases until, at a certain point, disappears and deemed to have undergone total deterioration. The reaction rate constants were derived from the slope of linear relationships and were used in the reaction kinetics of the degradation of CV and EY dyes (Fig. 11b). According to the results, the OSE-AgNPs were found to be the more effective catalyst for the dye degradation in comparison to AgNPs stabilized by other plant materials or AgNPs without a catalyst [37,78–80].

Here is a possible method that uses synthesized OSE-AgNPs in the presence of $NaBH_4$ to break down organic molecules, such as

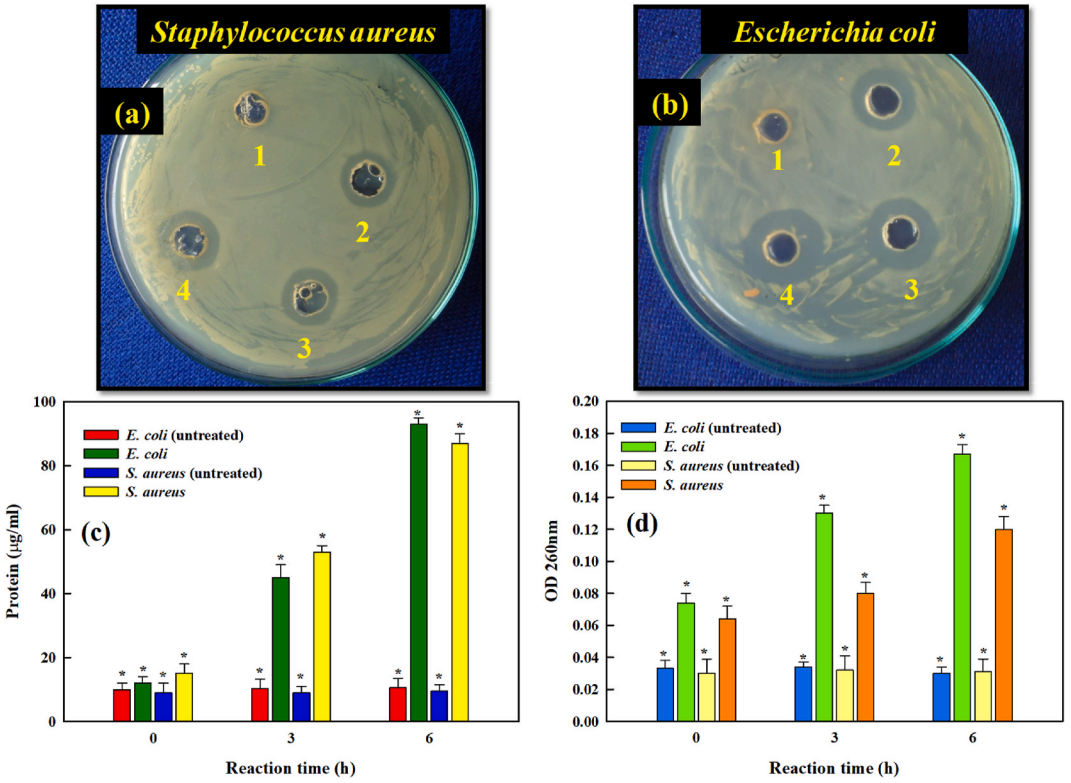

Fig. 8. Antibacterial activity of OSE-AgNPsagainst (a) *S. aureus*, (b) *E. coli*, (c) protein leakage, and (d) nucleic acid leakage. [1 = OSE; 2 = 20 μg/ml; 3 = 60 μg/ml; 4 = 100 μg/ml).

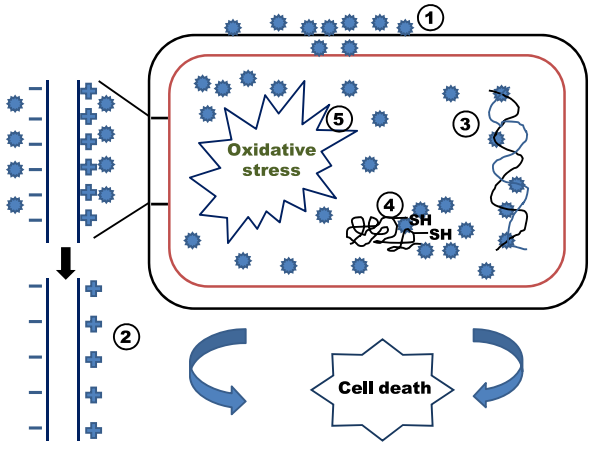

Fig. 9. Schematic illustration of proposed mode of action of nanoparticles (NPs).

dyes, antibiotics, and nitroaromatics. In particular, dyes were reduced and decomposed to make them stable and colourless [37,81]. The Langmuir-Hinshelwood representation was utilized to demonstrate the potential reaction mechanics in the catalytic breakdown of dyes with the assistance of AgNPs [82]. During the reduction process, $NaBH_4$ functions as both a hydrogen provider andan electron donor, affecting the pH of the entire solution. Because of high negative potential, AgNPs serve as an intermediary in the transfer of electrons between BH^{4-} ion and dyes [83]. The ion BH^{4-} from $NaBH_4$ and the dye molecules adsorbed on the surface of the AgNPs after $NaBH_4$ is added to a solution containing dye and AgNPs, leading to immediate electron and hydrogen transport. The next step of the catalytic reduction is the transfer of electrons from donor BH^{4-} to dye molecules, where AgNPs take the electrons from BH^{4-} ions and transfer them to the dye molecules. A significant amount of hydrogen supplied by $NaBH_4$ can cause dye hydrogenation in the presence of AgNPs.

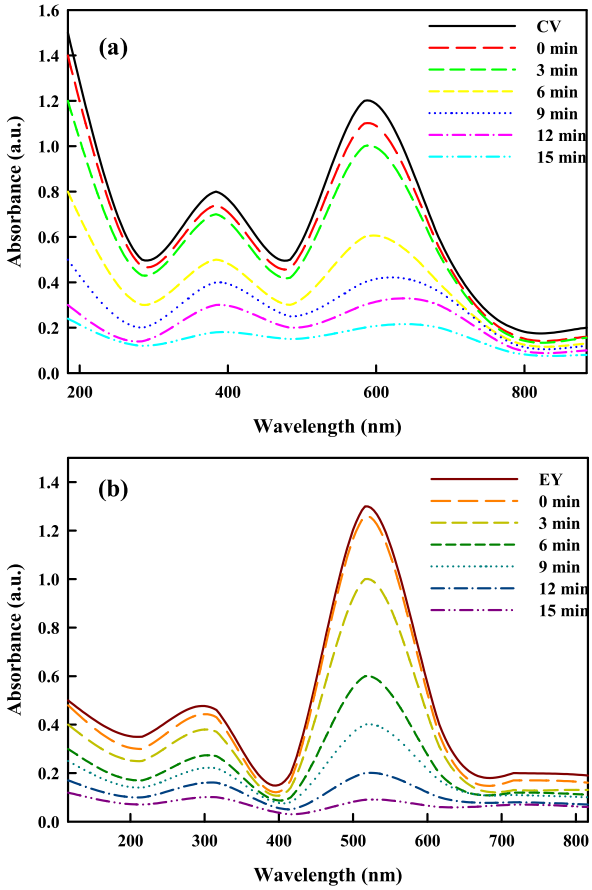

Fig. 10. Catalytic degradation of CV and EY dyes using OSE-AgNPs: UV–vis reduction profiles of (a) CV and (b) EY.

4. Conclusion

In conclusion, a straightforward and inexpensive production of AgNPs employing a green method and extract from *O. scolopendrina*as a stabilizing and reducing agent. UV–Visible spectroscopy, PL, FTIR, TEM, SEM, zeta potential and TGA analyses were used to examine and characterise the biosynthesizedOSE-AgNPs. The production of OSE-AgNPs supporting the SPR effect was evident from the UV–vis absorption spectra. The biological organic molecules used in the biomanufacture of OSE-AgNPs showed diverse functional groups to exhibit capping and reducing behaviour in their FTIR spectra. The synthesized OSE-AgNPs were confirmed by electron micrographs of TEM and SEM images to have an average size of 5–50 nm with a regular spherical morphology. In 15 minutes of reaction time, the biosynthesized OSE-AgNPs demonstrated significant catalytic activity in the entire degradation of CV & EY dyes. Because the OSE consisted of sufficient amount of biological organic molecules, the biosynthesized OSE-AgNPsexhibited notable bactericidal, DPPH and ABTS scavenging properties. Additionally, the OSE-AgNPsexhibited improved anti-diabetic action against enzymes α-amylase and α-glucosidase. The findings of the proposed work support the hypothesis that the biological organic molecules in OSE stabilized theOSE-AgNP synthesis and successfully displayed biological activities.

Author contribution statement

Ida Elizabeth George, Tijo Cherian: Conceived and designed the experiments; Performed the experiments; Contributed reagents, materials, analysis tools or data; Wrote the paper.

Syam Mohan: Conceived and designed the experiments; Analyzed and interpreted the data; Wrote the paper.

R. Mohanraju: Performed the experiments; Analyzed and interpreted the data; Wrote the paper.

C. Ragavendran: Analyzed and interpreted the data; Contributed reagents, materials, analysis tools or data; Wrote the paper.

Hamad Ghaleb Dailah, Rym Hassani, Hassan A. Alhazmi, Asaad Khalid: Analyzed and interpreted the data.

Funding statement

Dr Syam Mohan was supported by Deputyship for Research & Innovation, Ministry of Education in Saudi Arabia [ISP22-10].

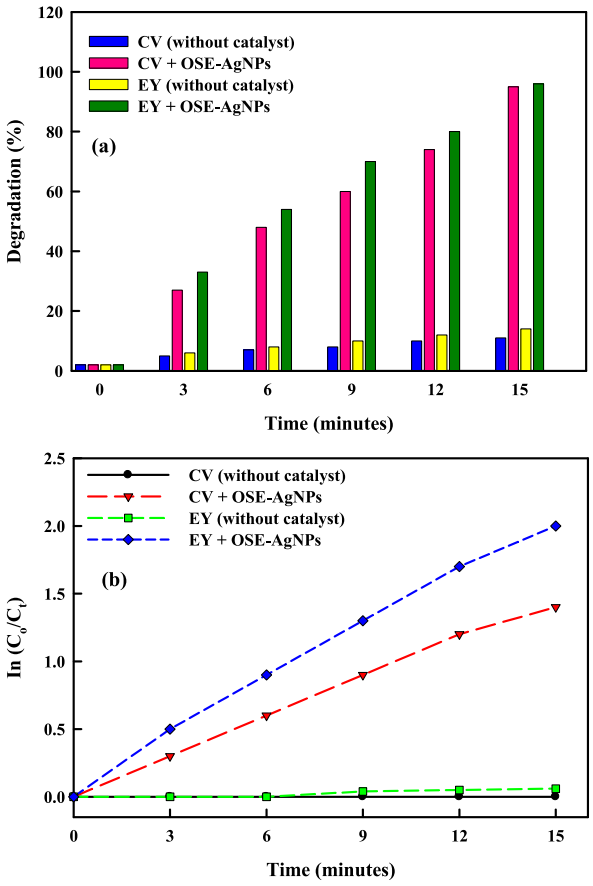

Fig. 11. Catalytic degradation of CV and EY dyes using OSE-AgNPs: (a) degradation efficiency plot and (b) kinetic plot for the estimation ofrate constants.

Data availability statement

Data included in article/supplementary material/referenced in article.

Declaration of interest's statement

The authors declare the following conflict of interests: The corresponding author is a member of Editorial board.

Acknowledgements

The authors extend their appreciation to the Deputyship for Research & Innovation, Ministry of Education in Saudi Arabia for funding this research work through the project number ISP22-10. The first author acknowledges Pondicherry University for providing infrastructural support.

References

[1] S. Albukhaty, et al., Production and characterization of biocompatible nanofibrous scaffolds made of β-sitosterol loaded polyvinyl alcohol/tragacanth gum composites, Nanotech 33 (2021), 085102.
[2] A.A. Alyamani, et al., Green fabrication of zinc oxide nanoparticles using Phlomis leaf extract: characterization and in vitro evaluation of cytotoxicity and antibacterial properties, Molecules 26 (2021) 6140.
[3] S.A. Fahmy, et al., Platinum nanoparticles: green synthesis and biomedical applications, Molecules 25 (21) (2020) 4981.
[4] H. Urena-Saborio, et al., Characterization and applications of silver nanoparticles-decorated electrospun nanofibers loaded with polyphenolic extract from rambutan (*Nephelium lappaceum*), Materialia 11 (2020), 100687.
[5] S.G. Eswaran, et al., Preparation of a portable calorimetry kit and one-step spectrophotometric nanomolar level detection of l-Histidine in serum and urine samples using sebacic acid capped silver nanoparticles, J. Sci. Adv. Mater. Devices 6 (2021) 100–107.
[6] S. Iravani, et al., Synthesis of silver nanoparticles: chemical, physical and biological methods, Res. Pharm. Sci. 9 (6) (2014) 385.
[7] M. Drahansky, et al., We are Intech Open, the World's Leading Publisher of Open Access Books Built by Scientists, for Scientists TOP 1 %, Intech, Vol. I, No. Tourism, 2016, p. 13.

[8] N. Govindan, et al., Effect of plant hormones on the production of biomass and lipid extraction for biodiesel production from microalgae *Chlorella* sp, J. Microbiol. Biotechnol. Food Sci. 9 (4) (2020).
[9] M. Behravan, et al., Facile green synthesis of silver nanoparticles using *Berberis vulgaris* leaf and root aqueous extract and its antibacterial activity, Int. J. Biol. Macromol. 124 (2019) 148–154.
[10] K. Chandhirasekar, et al., Plant-extract assisted green synthesis and its larvicidal activities of silver nanoparticles using leaf extract of *Citrus medica, Tagetes lemmonii*, and *Tarenna asiatica*, Mater. Lett. 287 (2021), 129265.
[11] H.V. Tran, et al., Silver nanoparticles as a bifunctional probe for label-free and reagentless colorimetric hydrogen peroxide chemosensor and cholesterol biosensor, J. Sci. Adv. Mater. Devices 5 (2020) 385–391.
[12] G. Ghoshal, M. Singh, Characterization of silver nano-particles synthesized using fenugreek leave extract and its antibacterial activity, Mater. Sci. Energy Technol. 5 (2022) 22–29.
[13] R. Javed, et al., Role of capping agents in the application of nanoparticles in biomedicine and environmental remediation: recent trends and future prospects, J. Nanobiotechnol. 18 (2020) 172.
[14] H. Karagoly, et al., Green synthesis, characterization, cytotoxicity, and antimicrobial activity of iron oxide nanoparticles using *Nigella sativa* seed extract, Green Process. Synth. 11 (2022) 254–265.
[15] S.N. Hawar, et al., Green synthesis of silver nanoparticles from *Alhagi graecorum* leaf extract and evaluation of their cytotoxicity and antifungal activity, J. Nanomater. 2022 (2022), 1058119.
[16] T. Pal, et al., Reversible formation and dissolution of silver nanoparticles in aqueous surfactant media, Langmuir 13 (1997) 1481–1485.
[17] S.G. Keskin, et al., Synthesis, characterization, coordination chemistry, and luminescence studies of copper, silver, palladium, and platinum complexes with a phosphorus/nitrogen/phosphorus ligand, Inorg. Chim. Acta. 486 (2019) 200–212.
[18] J. Chen, et al., Konjac glucomannan reduced-stabilized silver nanoparticles for mono-azo and di-azo contained wastewater treatment, Inorg. Chim. Acta. 515 (2021), 120058.
[19] D. Rawat, et al., Ecotoxic potential of a presumably nontoxic azo dye, Ecotoxicol. Environ. Saf. 148 (2018) 528–537.
[20] L. David, B. Moldovan, Green synthesis of biogenic silver nanoparticles for efficient catalytic removal of harmful organic dyes, Nanomaterials 10 (2020) 202.
[21] V. Katheresan, et al., Efficiency of various recent wastewater dye removal methods: a review, J. Environ. Chem. Eng. 6 (2018) 4676–4697.
[22] E.J. Rupa, et al., Synthesis of a zinc oxide nanoflower photocatalyst from Sea buckthorn fruit for degradation of industrial dyes in wastewater treatment, Nanomaterials 9 (2019) 1692.
[23] C. Raghunathan, et al., A Guide to Common Echinoderms of Andaman and Nicobar Islands, Zoological Survey India, Kolkata, 2013, pp. 1–210.
[24] D. Inbakandan, et al., Ultrasonic-assisted green synthesis of flower like silver nanocolloids using marine sponge extract and its effect on oral biofilm bacteria and oral cancer cell lines, Microb. Pathog. 99 (2016) 135–141.
[25] T. Cherian, et al., *Cymbopogon citratus* functionalized green synthesis of CuO nanoparticles: novel prospects as antibacterial and antibiofilm agents, Biomolecules 10 (2020) 169.
[26] T. Cherian, et al., Green chemistry based gold nanoparticles synthesis using the marine bacterium *Lysinibacillus odysseyi* PBCW2 and their multitudinous activities, Nanomaterials 12 (2022) 2940.
[27] S.K. Lee, et al., Evaluation of the antioxidant potential of natural products, Comb. Chem. High Throughput Screen. 1 (1998) 35–46.
[28] A.O. Ademiluyi, G. Oboh, Soybean phenolic-rich extracts inhibit key-enzymes linked to type 2 diabetes (α-amylase and α-glucosidase) and hypertension (angiotensin I converting enzyme) in vitro, Exp. Toxicol. Pathol. 65 (3) (2013) 305–309.
[29] L. Jeremia, Inhibitory effects of five medicinal plants on rat alpha-glucosidase: comparison with their effects on yeast alpha-glucosidase, J. Med. Plants Res. 5 (2014) 2863–2867.
[30] S.-H. Kim, et al., Antibacterial activity of silver-nanoparticles against *Staphylococcus aureus* and *Escherichia coli*, Microbiol.Biotechnol.Lett. 39 (2011) 77–85.
[31] A. Álvarez-Ordóñez, et al., Antibacterial activity and mode of action of a commercial citrus fruit extract, J. Appl. Microbiol. 115 (2013) 50–60.
[32] M. Vinosha, et al., Biogenic synthesis of gold nanoparticles from *Halymenia dilatata* for pharmaceutical applications: antioxidant, anti-cancer and antibacterial activities, Process Biochem. 85 (2019) 219–229.
[33] M.K. Panda, et al., Green synthesis of silver nanoparticles and its potential effect on phytopathogens, Mater. Today Proc. 35 (2) (2021) 233–238.
[34] P. Bhuyar, et al., Synthesis of silver nanoparticles using marine macroalgae *Padina* sp. and its antibacterial activity towards pathogenic bacteria, Beni-Suef Uni, J. Basic Appl. Sci. 9 (3) (2020).
[35] A. Nabikhan, et al., Synthesis of antimicrobial silver nanoparticles by callus and leaf extracts from saltmarsh plant, *Sesuvium portulacastrum* L, Colloids Surf. B Biointerfaces 79 (2) (2010) 488–493.
[36] C.R. Resmi, et al., Green synthesis of silver nanoparticles using *Azadirachta indica* leaves extract and evaluation of antibacterial activities, Int. J. Adv. Biol. Res. 4 (2014) 300–303.
[37] S. Seekonda, R. Rani, Eco-friendly synthesis, characterization, catalytic, antibacterial, antidiabetic, and antioxidant activities of *Embelia robusta* seeds extract stabilized AgNPs, J. Sci.: Adv. Mat. Dev. 7 (2022), 100480.
[38] R. Sarkar, et al., Green synthesis of silver nanoparticles and its optical properties, Dig, J. Nanomat. Biostruct. 5 (2010) 491–496.
[39] L. D'Souza, et al., Use of Fourier transform infrared (FTIR) spectroscopy to study cadmium-induced changes in *Padina tetrastromatica* (Hauck), Anal. Chem. Insights 3 (2008) 135–143.
[40] M. Puchalski, et al., The study of silver nanoparticles by scanning electron microscopy, energy dispersive X-ray analysis and scanning tunnelling microscopy, Mater. Sci. Pol. 25 (2) (2007) 473–478.
[41] P. Kumar, et al., Seaweed-mediated biosynthesis of silver nanoparticles using *Gracilaria corticata* for its antifungal activity against *Candida* spp, Appl. Nanosci. 3 (6) (2013) 495–500.
[42] S. Kannan, FT-IR and EDS analysis of the seaweeds *Sargassum wightii* and *Gracilaria corticata* (red algae), Int. J. Curr. Microbiol. Appl. Sci. 3 (4) (2014) 341–351.
[43] S.G. Balwe, et al., Green synthesis and characterization of silver nanoparticles (AgNPs) from extract of plant Radix Puerariae: an efficient and recyclable catalyst for the construction of pyrimido[1,2-b] indazole derivatives under solvent-free conditions, Catal. Commun. 99 (2017) 121–126.
[44] J.S. Kim, et al., Antimicrobial effects of silver nanoparticles, Nanomed. Nanotechnol. Biol. Med. 3 (1) (2007) 95–101.
[45] H. Bönnemann, R.M. Richards, Nanoscopic metal particles – synthetic methods and potential applications, Eur. J. Inorg. Chem. 10 (2001) 2455.
[46] N. Wangoo, et al., Zeta potential based colorimetric immunoassay for the direct detection of diabetic marker HbA1c using gold nanoprobes, Chem. Commun. 46 (31) (2010) 5755–5757.
[47] S. Singh, et al., Structural, thermal, zeta potential and electrical properties of disaccharide reduced silver nanoparticles, J. Mater. Sci. Mater. Electron. 25 (9) (2014) 3747–3752.
[48] A.M.E. Badawy, et al., Impact of environmental conditions (pH, ionic strength, and electrolyte type) on the surface charge and aggregation of silver nanoparticles suspensions, Environ. Sci. Technol. 44 (2010) 1260–1266.
[49] C.G. Kumar, S.K. Mamidyala, Extracellular synthesis of silver nanoparticles using culture supernatant of *Pseudomonas aeruginosa*, Colloids Surf. B Biointerfaces 84 (2011) 462–466.
[50] L. Salvioni, et al., Negatively charged silver nanoparticles with potent antibacterial activity and reduced toxicity for pharmaceutical preparations, Int. J. Nanomed. 12 (2017) 2517.
[51] Y. Khane, et al., Green synthesis of silver nanoparticles using aqueous citrus limon zest extract: characterization and evaluation of their antioxidant and antimicrobial properties, Nanomaterials 12 (2022) (2013).
[52] S. Hemmati, et al., Green synthesis and characterization of silver nanoparticles using *Fritillaria* flower extract and their antibacterial activity against some human pathogens, Polyhedron 158 (2019) 8–14.
[53] V. Huong Thi Lan, N.T. Nguyen, Green synthesis, characterization and antibacterial activity of silver nanoparticles using *Sapindus mukorossi* fruit pericarp extract, Mater. Today Proc. 42 (1) (2020) 88–93.

[54] Z.H. Mbhele, et al., Fabrication and characterization of silver–polyvinyl alcohol nanocomposites, Chem. Mater. 15 (26) (2003) 5019–5024.
[55] K. Chokshi, et al., Green synthesis, characterization and antioxidant potential of silver nanoparticles biosynthesized from de-oiled biomass of thermotolerant oleaginous microalgae *Acutodesmus dimorphus*, RSC Adv. 6 (76) (2016) 72269–72274.
[56] I. Gulcin, The antioxidant and radical scavenging activities of black pepper (*Piper nigrum*) seeds, Int. J. Food Sci. Nutr. 56 (2005) 491–499.
[57] R. Vennilaraj, et al., Green synthesis of silver nanoparticles from *Cleistanthus collinus* leaf extract and their biological effects, Int. J. Chem. 34 (2013) 1103–1107.
[58] N. Muniyappan, N. Nagarajan, Green synthesis of silver nanoparticles with *Dalbergia spinosa* leaves and their applications in biological and catalytic activities, Process Biochem. 49 (2014) 1054–1061.
[59] A. Saravanakumar, et al., Biosynthesis of silver nanoparticles using *Cassia tora* leaf extract and its antioxidant and antibacterial activities, J. Ind. Eng. Chem. 28 (2015) 277–281.
[60] N. Bala, et al., Green synthesis of zinc oxide nanoparticles using *Hibiscus subdariffa* leaf extract: effect of temperature on synthesis, anti-bacterial activity and anti-diabetic activity, RSC Adv. 5 (2015) 4993–5003.
[61] D. Mahendiran, et al., Biosynthesis of zinc oxide nanoparticles using plant extracts of *Aloevera* and *Hibiscus sabdariffa*: phytochemical, antibacterial, antioxidant and anti-proliferative studies, BioNanoSci 7 (2017) 530–545.
[62] V. Vignesh, et al., Green synthesis of biogenic silver nanomaterials using *Raphanus sativus* extract, effects of stabilizers on the morphology, and their antimicrobial activities, Physicochem. Eng. Aspects 12 (2013) 37–46.
[63] D. ArumaiSelvan, et al., Garlic, green tea and turmeric extracts-mediated green synthesis of silver nanoparticles: phytochemical, antioxidant and in vitro cytotoxicity studies, J. Photochem. Photobiol. B Biol. 180 (2018) 243–252.
[64] M. Gangwar, et al., Antioxidant capacity and radical scavenging effect of polyphenol rich *Mallotus philippenensis* fruit extract on human erythrocytes: an in vitro study, Sci. World J. (279451) (2014) 1–12.
[65] P. Dauthal, M. Mukhopadhyay, In-vitro free radical scavenging activity of biosynthesized gold and silver nanoparticles using *Prunus armeniaca* (apricot) fruit extract, J. Nano Res. 15 (1) (2013) 1366.
[66] A.K. Mittal, et al., Biosynthesis of silver nanoparticles: elucidation of prospective mechanism and therapeutic potential, J. Colloid Interface Sci. 415 (2014) 39–47.
[67] D. Nallappan, et al., Green biosynthesis, antioxidant, antibacterial, and anticancer activities of silver nanoparticles of *Luffa acutangula* leaf extract, Bio. Med. Res. Inter. 5125681 (2021) 1–28.
[68] P.M. Sales, et al., α-Amylase inhibitors: a review of raw material and isolated compounds from plant source, J. Pharm. Pharmaceut. Sci. 15 (2012) 141–183.
[69] K. Balan, et al., Antidiabetic activity of silver nanoparticles from green synthesis using *Lonicera japonica* leaf extract, RSC Adv. 6 (2016) 40162–40168.
[70] F.K. Alsammarraie, et al., Green synthesis of silver nanoparticles using turmeric extracts and investigation of their antibacterial activities, Colloids Surf. B Biointerfaces 171 (2018) 398–405.
[71] Y.N. Slavin, et al., Metal nanoparticles: understanding the mechanisms behind antibacterial activity, J. Nanobiotechnol. 15 (1) (2017) 1–20.
[72] M. Darroudi, et al., Gelatinous silver colloid nanoparticles: synthesis, characterization, and their antibacterial activity, J. Optoelectron. Adv. Mater. 16 (1–2) (2014) 182–187.
[73] X. Liang, et al., Preparation and antibacterial activities of polyaniline/Cu0.05Zn0.95O nanocomposites, Dalton Trans. 41 (9) (2012) 2804–2811.
[74] I. Sondi, B. Salopek-Sondi, Silver nanoparticles as antimicrobial agent: a case study on *E. coli* as a model for Gram-negative bacteria, J. Colloid Interface Sci. 275 (2004) 177–182.
[75] S. Mingyu, et al., Effects of nano-anatase TiO_2 on absorption, distribution of light, and photoreduction activities of chloroplast membrane of spinach, Biol. Trace Elem. Res. 118 (2007) 120–130.
[76] A.E. Nel, et al., Understanding biophysicochemical interactions at nano-biointerface, Nat. Mater. 8 (2009) 543–557.
[77] C. Marmambio-Jones, E.M.V. Hoek, A review of the antibacterial effects of silver nanomaterials and potential implications for human health and the environment, J. Nanopart.Res. 12 (2010) 1531.
[78] K. Chand, et al., Green synthesis, characterization and photocatalytic application of silver nanoparticles synthesized by various plant extracts, Arab. J. Chem. 13 (2020) 8248–8261.
[79] M.I. Al-Zaban, et al., Catalytic degradation of methylene blue using silver nanoparticles synthesized by honey, Saudi J. Biol. Sci. 28 (2021) 2007–2013.
[80] S. Li, et al., Photocatalytic degradation of antibiotics using a novel $Ag/Ag_2S/Bi_2MoO_6$ plasmonic p-n heterojunction photocatalyst: mineralization activity, degradation pathways and boosted charge separation mechanism, Chem. Eng. J. 415 (2021), 128991.
[81] V. Suvith, D. Philip, Catalytic degradation of methylene blue using biosynthesized gold and silver nanoparticles, Spectrochim. Acta Part A Mol. Biomol. Spectrosc. 118 (2014) 526–532.
[82] A. Panacek, et al., Polyacrylate-assisted size control of silver nanoparticles and their catalytic activity, Chem. Mater. 26 (2014) 1332–1339.
[83] T.N.J.I. Edison, et al., *Caulerpa racemosa*: green synthesis of silver nanoparticles using *Terminalia cuneata* and its catalytic action in reduction of direct yellow-12 dye, Spectrochim. Acta 161 (2016) 122–129.